MORGAN & CLAYPOOL PUBLISHERS

The Transfer-Matrix Method in Electromagnetics and Optics

Tom G. Mackay
Akhlesh Lakhtakia

SYNTHESIS LECTURES ON ELECTROMAGNETICS
Series Editor: Akhlesh Lakhtakia, *The Pennsylvania State University*

The Transfer-Matrix Method in Electromagnetics and Optics

Synthesis Lectures on Electromagnetics

The Transfer-Matrix Method in Electromagnetics and Optics
Tom G. Mackay and Akhlesh Lakhtakia
2020

The Transfer-Matrix Method in Electromagnetics and Optics

Tom G. Mackay and Akhlesh Lakhtakia

www.morganclaypool.com

ISBN: 9781681737928 paperback
ISBN: 9781681737935 ebook
ISBN: 9781681737942 hardcover

DOI 10.2200/S00993ED1V01Y202002EMA001

A Publication in the Morgan & Claypool Publishers series
SYNTHESIS LECTURES ON ELECTROMAGNETICS

Lecture #1
Series ISSN
ISSN pending.

The Transfer-Matrix Method in Electromagnetics and Optics

Tom G. Mackay
University of Edinburgh

Akhlesh Lakhtakia
The Pennsylvania State University

SYNTHESIS LECTURES ON ELECTROMAGNETICS #1

MORGAN & CLAYPOOL PUBLISHERS

ABSTRACT

The transfer-matrix method (TMM) in electromagnetics and optics is a powerful and convenient mathematical formalism for determining the planewave reflection and transmission characteristics of an infinitely extended slab of a linear material. While the TMM was introduced for a homogeneous uniaxial dielectric-magnetic material in the 1960s, and subsequently extended for multilayered slabs, it has more recently been developed for the most general linear materials, namely bianisotropic materials. By means of the rigorous coupled-wave approach, slabs that are periodically nonhomogeneous in the thickness direction can also be accommodated by the TMM. In this book an overview of the TMM is presented for the most general contexts as well as for some for illustrative simple cases. Key theoretical results are given; for derivations, the reader is referred to the references at the end of each chapter. Albums of numerical results are also provided, and the computer code used to generate these results are provided in an appendix.

KEYWORDS

transfer matrix, bianisotropy, periodic nonhomogeneity, rigorous coupled-wave approach, reflectance, transmittance, slab, matrix ordinary differential equation

Dedicated to the ethic of eco-responsibility championed by Rachel Carson, Wangari Maathai, and Greta Thunberg

Contents

Preface

The transfer-matrix method (TMM) for linear electromagnetics and optics came into existence during the 1960s. Initiated in the 1966 doctoral thesis of Jean Billard for a homogeneous uniaxial dielectric-magnetic material, application of the TMM for multilayered slabs became popular after the publication of three papers of Dwight W. Berreman from 1970–1973. The rigorous coupled-wave approach widely used to solve grating problems emerged in the early 1980s from the papers of M. G. Moharam and Thomas K. Gaylord, its implementation requiring the TMM for electrically thin slabs.

In this book on the TMM, only key results are given, full details of derivations of these results being available in the references listed at the end of each chapter. The intended readership comprises graduate students and researchers, seeking a concise survey of the state-of-the-art about the TMM for electromagnetics and optics. A familiarity with undergraduate-level electromagnetic theory is assumed. SI units are used throughout.

Tom G. Mackay, Edinburgh, Scotland
Akhlesh Lakhtakia, University Park, PA, USA
January 2020

Acknowledgments

Every year, both of us learn more about electromagnetic theory and applications, not only through our own research but also by reviewing manuscripts, reading publications, attending seminars and conferences, and interacting with other researchers. We take joy in acknowledging our debt of gratitude to currently active colleagues worldwide as well as those who carried the beacons of science before us.

We especially thank Kevin Vynck of Institut d'Optique d'Aquitaine (Talence, France) for locating the Ph.D. thesis of Jean Billard, whose seminal contribution to the transfer-matrix method has remained obscure for five decades.

Akhlesh Lakhtakia thanks Faiz Ahmad, Tom H. Anderson, Francisco Chiadini, Benjamin J. Civiletti, Jhuma Dutta, Muhammad Faryad, Vincenzo Fiumara, Peter B. Monk, John A. Polo Jr., S. Anantha Ramakrishna, Antonio Scaglione, Mikhail V. Shuba, Manuel E. Solano, Vijayakumar C. Venugopal, and Fei Wang for research discussions that either directly or indirectly shaped this book. He also thanks the US National Science Foundation for two grants (DMR-1125591 and DMS-1619901), the Charles Godfrey Binder Endowment at The Pennsylvania State University for ongoing support of his research from 2006, and the Trustees of The Pennsylvania State University as well as the Otto Mønsted Foundation for enabling a sabbatical leave of absence at the Danish Technical University in Fall 2019. Tom Mackay acknowledges the support of EPSRC grant EP/S00033X/1.

We thank our families for their loving support and the staff of Morgan & Claypool for producing this book.

CHAPTER 1

Introduction

The transfer-matrix method (TMM) in electromagnetics and optics is a mathematically convenient formalism for determining the planewave reflection and transmission characteristics of an infinitely extended slab of a linear material. The direction of propagation and the polarization state of the incident plane wave can be arbitrary. This arbitrariness allows the TMM to be useful for the illumination of the slab by a finite source located at a finite distance from either of the two faces of the slab, because the time-harmonic fields radiated by that source can be expressed as an angular spectrum of plane waves [1]. The slab may be spatially homogeneous in the thickness direction or not. In the latter case, the slab may be continuously nonhomogeneous as for certain sculptured thin films [2] or the slab may be piecewise homogeneous in which case it is regarded as a multilayered slab [3, 4]. In a multilayered slab, the interface of any two adjacent constituent layers may be planar or periodically corrugated [5]. Finally, the materials in a slab may be of the most general linear type, i.e., bianisotropic materials [6].

Consider a bilayered slab occupying the region $0 < z < d$. Both constituent layers are homogeneous, have infinite extent along the x and y axes, and have finite thickness (along the z axis), as shown in Fig. 1.1(a). The interface of the two layers is planar and is parallel to both exposed faces of the bilayer. If a plane wave is considered incident on the bilayered slab, there must also exist a reflected plane wave and a transmitted plane wave. The TMM uses two 4×4 matrixes, one for each constituent layer in the bilayered slab, to relate the complex-valued amplitudes of the electric field phasor of the reflected and transmitted plane waves to the complex-valued amplitude of the electric field phasor of the incident plane wave. These 4×4 matrixes are called *transfer matrixes*.

Suppose the interface of the two constituent layers is periodically corrugated along the x axis and the direction of propagation of the incident plane wave lies wholly in the xz plane, as shown in Fig. 1.1(b). Then, the reflected electromagnetic field comprises an infinite number of distinct plane waves. These reflected plane waves are labeled $0, \pm 1, \pm 2, \ldots$. The reflected plane wave labeled 0 is called *specular*, the remaining ones being *nonspecular*. Only some of the nonspecular plane waves in the reflected field can transport energy an infinite distance from the bilayered slab. The transmitted electromagnetic field also comprises a specular plane wave (labeled 0) and an infinite number of nonspecular plane waves (labeled other than 0). Again, only some of the nonspecular plane waves in the transmitted field can transport energy an infinite distance from the bilayered slab. The TMM uses two $4(2M_t + 1) \times 4(2M_t + 1)$ matrixes, one for each constituent layer in the bilayered slab, to relate the complex-valued amplitudes of the

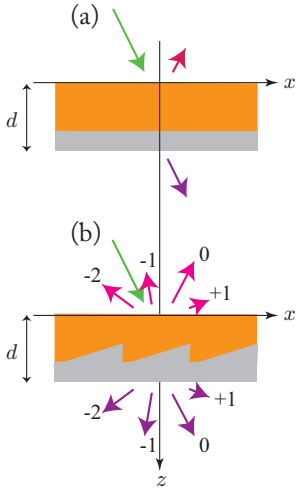

Figure 1.1: (a) Specular reflection and transmission of a plane wave incident on a bilayered slab wherein all interfaces are planar and parallel to each other. (b) Specular (labeled 0) and nonspecular (labeled other than 0) reflection and transmission when the internal interface in a bilayer is periodically corrugated along the x axis. The nonspecular modes are infinite in number, but only a few can propagate energy an infinite distance from the bilayered slab.

electric field phasors of the reflected and transmitted plane waves to the complex-valued amplitude of the electric field phasor of the incident plane wave, with the integer $M_t > 0$ being sufficiently large.

When the interface of the two constituent layers is periodically corrugated along both the x and y axes, the TMM uses two $4(2\tau_t + 1) \times 4(2\tau_t + 1)$ matrixes, one for each layer in the bilayered slab, where $\tau_t = M_t(N_t + 1) + N_t(M_t + 1)$ and the integers $M_t > 0$ and $N_t > 0$ are sufficiently large.

1.1 BRIEF HISTORY OF TMM

Before the advent of the TMM, recursive schemes had been formulated and implemented for multilayered slabs comprising planar layers of isotropic dielectric materials [7–10]. If the incident plane wave is linearly polarized, the reflected and transmitted plane waves then have the same polarization state as the incident plane wave. These schemes can be extended to incorporate periodically corrugated interfaces [11, 12], but become cumbersome [13] when the reflected and transmitted plane waves can have both co-polarized and cross-polarized components. That happens when: (i) materials more complicated than isotropic dielectric-magnetic materials [6, 14] are involved, and/or (ii) the direction of propagation of the incident plane wave has a nonzero component along the y axis and an interface is periodically corrugated along the x axis, and/or

(iii) when the interface is periodically corrugated along both the x and y axes [5, 15, 16]. The TMM is very convenient when such issues must be tackled.

When a linearly polarized plane wave is incident on a slab of an isotropic dielectric material, the electromagnetic fields induced inside it can be decomposed into two plane waves, one propagating toward one face of the slab and the other propagating toward the other face. Both of these plane waves have the same polarization state as the incident plane wave. The amplitudes of the electric field phasors of the induced plane waves can be used to formulate a 2×2 matrix, which can be used to develop a matrix formulation [17–21] for multilayered slabs with planar interfaces. This matrix formulation can be extended to encompass anisotropic dielectric materials [12], but the extension is inelegant and definitely cumbersome.

For any time-harmonic electromagnetic field in a source-free region occupied by any homogeneous isotropic dielectric-magnetic medium, the derivative $(\partial/\partial z)\left[\left(\underline{u}_x\underline{u}_x + \underline{u}_y\underline{u}_y\right) \cdot \underline{E}(\underline{r},\omega)\right]$ can be written in terms of the x- and y-directed components of $\underline{H}(\underline{r},\omega)$ and their derivatives with respect to x and y, where $\underline{r} = x\underline{u}_x + y\underline{u}_y + z\underline{u}_z$ is the position vector with $\left\{\underline{u}_x, \underline{u}_y, \underline{u}_z\right\}$ as the triad of Cartesian unit vectors, and ω is the angular frequency. Likewise, the derivative $(\partial/\partial z)\left[\left(\underline{u}_x\underline{u}_x + \underline{u}_y\underline{u}_y\right) \cdot \underline{H}(\underline{r},\omega)\right]$ can be written in terms of the x- and y-directed components of $\underline{E}(\underline{r},\omega)$ and their derivatives with respect to x and y [22]. These relationships can be extended to source-free regions occupied by homogeneous bianisotropic materials [23]. Accordingly, if the field phasors are expressed as

$$\left.\begin{aligned} \underline{E}(\underline{r},\omega) &= \underline{e}(z,\omega)\, \exp\left[iq(x\cos\psi + y\sin\psi)\right] \\ \underline{H}(\underline{r},\omega) &= \underline{h}(z,\omega)\, \exp\left[iq(x\cos\psi + y\sin\psi)\right] \end{aligned}\right\}, \tag{1.1}$$

with auxiliary phasors

$$\left.\begin{aligned} \underline{e}(z,\omega) &= e_x(z,\omega)\underline{u}_x + e_y(z,\omega)\underline{u}_y + e_z(z,\omega)\underline{u}_z \\ \underline{h}(z,\omega) &= h_x(z,\omega)\underline{u}_x + h_y(z,\omega)\underline{u}_y + h_z(z,\omega)\underline{u}_z \end{aligned}\right\}, \tag{1.2}$$

the 4×4 matrix ordinary differential equation

$$\frac{d}{dz}\left[\underline{f}(z,\omega)\right] = i\left[\underline{\underline{P}}(\omega)\right] \cdot \left[\underline{f}(z,\omega)\right] \tag{1.3}$$

is obtained. Herein, $q(\underline{u}_x\cos\psi + \underline{u}_y\sin\psi)$ is the transverse wave vector with $\psi \in [0, 2\pi)$ as an angle, the 4-column vector

$$\left[\underline{f}(z,\omega)\right] = \begin{bmatrix} e_x(z,\omega) \\ e_y(z,\omega) \\ h_x(z,\omega) \\ h_y(z,\omega) \end{bmatrix}, \tag{1.4}$$

while the 4×4 matrix $\left[\underline{\underline{P}}(\omega)\right]$ is specified in (2.49).

Equation (1.3) is the bedrock of the TMM. It was formulated and solved for propagation in a uniaxial dielectric-magnetic material by Billard in 1966 [24]. Shortly thereafter, Teitler and Henvis [25] formulated and solved (1.3) for a slab of an anisotropic dielectric material, but then they reverted to the 2×2-matrix formalism of Abelès that had originated two decades earlier [20]. However, Berreman persevered with 4×4 matrixes, first for slabs of cholesteric liquid crystals [26] and then for slabs of homogeneous bianisotropic materials [27].

Early attempts to apply the TMM to a slab composed of a continuously nonhomogeneous material must be viewed with caution. Although Berreman [26] correctly applied a numerical technique to solve (1.3) for a cholesteric liquid crystal of finite thickness, Equation (6) in Ref. 28 is incorrect [29]. A piecewise-uniform approximation provides a convenient path to handle slabs of continuously nonhomogeneous materials [30, 31], but other numerical techniques also exist [32, 33]. The TMM has also been developed to accommodate anisotropic [15] and bianisotropic [5, 16] layers with periodically corrugated interfaces.

1.2 APPLICATIONS OF TMM

A commonplace experimental configuration, i.e., a light beam incident on a slab, provides the backdrop for the TMM. A beam of large width in relation to the wavelength can be approximated by a plane wave [1]. Accordingly, the TMM is useful for a host of practical applications.

If the slab is a single layer of a homogeneous or nonhomogeneous material, the TMM can be harnessed with ellipsometry measurements [34, 35] to characterize the optical properties of the slab material. Furthermore, the TMM can be exploited to aid the design of optical components such as Bragg mirrors, antireflection coatings, waveplates, and polarization converters [35–37].

Another major area of TMM application for multilayered slabs lies in the analysis of surface waves that are guided by the planar interface of two dissimilar materials [5, 38]. For example, in the case of spatially homogeneous constituent layers, Dyakonov surface waves [39–41] can be excited at the interface of two dielectric constituent layers provided that one of them is anisotropic, while surface-plasmon-polariton waves [42, 43] can be excited at the interface of two isotropic constituent layers provided that one of them is metallic. If one (or more) of the constituent layers is periodically nonhomogeneous in the thickness direction, then Tamm surface waves [44, 45] can be excited at the interface of two isotropic constituent layers or Dyakonov–Tamm surface waves [46, 47] can be excited provided that one of the constituent layers is anisotropic. Composite guided waves excited in a multilayered slab can also be identified using the TMM [48].

If the interfaces of adjacent constituent layers in a multilayered slab are planar, the slab provides an appropriate model for the analysis of prism-coupled excitation of surface waves, as arises in the Turbadar–Kretschmann–Raether [49–51] and Turbadar–Otto [52] configurations. On the other hand, if an interface of two adjacent constituent layers is periodically corrugated,

then the TMM can be harnessed to analyze surface waves that are excited in the grating-coupled configuration [42, 53, 54].

The versatility of the TMM extends to the incorporation of a layer of a topological insulator [55, 56] in a slab through suitable jump conditions across the two faces of that layer [57]. Also, infinitely extended graphene [58] can be incorporated through a jump condition across it [59].

1.3 OVERVIEW

The TMM is presented in full generality in this book. Chapter 2 provides the prerequisite electromagnetic theory concerning linear materials; bianisotropic materials and specializations thereof are described, and the 4×4-matrix formulation for planewave propagation in such materials is introduced. The TMM for a slab with adjacent constituent layers that have planar interfaces is presented in Chapter 3. The material of each constituent layer is spatially homogeneous and bianisotropic in general. By means of a piecewise-uniform approximation, the same formalism can be applied to a bianisotropic slab which is spatially nonhomogeneous in the thickness direction. The TMM formalism of Chapter 3 is extended in Chapter 4 wherein a multilayered slab containing two adjacent constituent layers with a doubly periodic interface is considered; as in Chapter 3, the constituent layers in Chapter 4 are spatially homogeneous and bianisotropic. In order to highlight the key features of the TMM for the simplest scenario, the TMM is given in Chapter 5 for a multilayered slab made of isotropic dielectric materials, and the constituent layers can have either planar interfaces or singly periodic interfaces. Chapter 6 comprises some closing remarks. A short overview of 3×3 dyadics is provided in Appendix A; for further details, readers are referred elsewhere [60]. Mathematica™ codes used to generate the numerical results presented in Chapters 3 and 5 are provided in Appendix B.

In the notation adopted, 3-vectors are underlined once while 3×3 dyadics [60] are double underlined. Matrixes are doubled underlined and enclosed in square brackets; and n-vectors where $n > 3$ are underlined once and enclosed in square brackets. The identity 3×3 dyadic is denoted by $\underline{\underline{I}} = \underline{u}_x \underline{u}_x + \underline{u}_y \underline{u}_y + \underline{u}_z \underline{u}_z$ and the null 3×3 dyadic by $\underline{\underline{0}}$. The real and imaginary parts of complex quantities are delivered by the operators $\mathrm{Re}\{\bullet\}$ and $\mathrm{Im}\{\bullet\}$, respectively. The complex conjugate of a complex-valued scalar ζ is denoted by ζ^*. The symbols ε_0 and μ_0 represent the permittivity and permeability of free space, respectively. The free-space wavenumber is denoted by $k_0 = \omega\sqrt{\varepsilon_0 \mu_0}$, the wavelength in free space by $\lambda_0 = 2\pi/k_0$, and the intrinsic impedance of free space by $\eta_0 = \sqrt{\mu_0/\varepsilon_0}$. SI units are adopted throughout.

1.4 REFERENCES

[1] Clemmow, P. C. 1966. *The Plane Wave Spectrum Representation of Electromagnetic Fields* (New York, Pergamon Press). DOI: 10.1109/9780470546598. 1, 4

[2] Lakhtakia, A. and Messier, R. 2005. *Sculptured Thin Films: Nanoengineered Morphology and Optics* (Bellingham, WA, SPIE Press). DOI: 10.1117/3.585322. 1

[3] Huxley, A. F. 1968. A theoretical treatment of the reflexion of light by multilayer structures, *J. Exp. Biol.*, 48:227–245. 1

[4] Yeh, P. 1980. Optics of anisotropic layered media: A new 4 × 4 matrix algebra, *Surf. Sci.*, 96:41–53. DOI: 10.1016/0039-6028(80)90293-9. 1

[5] Polo, J. A., Jr., Mackay, T. G., and Lakhtakia, A. 2013. *Electromagnetic Surface Waves: A Modern Perspective* (Waltham, MA, Elsevier). 1, 3, 4

[6] Mackay, T. G. and Lakhtakia, A. 2019. *Electromagnetic Anisotropy and Bianisotropy: A Field Guide*, 2nd ed. (Singapore, World Scientific). DOI: 10.1142/11351. 1, 2

[7] Rouard, P. 1937. Études des propriétés optiques des lames métalliques très minces, *Ann. Phys.*, 11:291–384, Paris. DOI: 10.1051/anphys/193711070291. 2

[8] Vašiček, A. 1947. The reflection of light from glass with double and multiple films, *J. Opt. Soc. Am.*, 37:954–964. DOI: 10.1364/josa.37.000623. 2

[9] Crook, A. W. 1948. The reflection and transmission of light by any system of parallel isotropic films, *J. Opt. Soc. Am.*, 38:623–634. DOI: 10.1364/josa.38.000954. 2

[10] Parratt, L. G. 1954. Surface studies of solids by total reflection of X-rays, *Phys. Rev.*, 95:359–369. DOI: 10.1103/physrev.95.359. 2

[11] Cain, W. N., Varadan, V. K., Varadan, V. V., and Lakhtakia, A. 1986. Reflection and transmission characteristics of a slab with periodically varying surfaces, *IEEE Trans. Antennas Propagat.*, 34:1159–1163. DOI: 10.1109/tap.1986.1143949. 2

[12] Abdulhalim, I. 1999. 2 × 2 Matrix summation method for multiple reflections and transmissions in a biaxial slab between two anisotropic media, *Opt. Commun.*, 163:9–14. DOI: 10.1016/s0030-4018(99)00129-7. 2, 3

[13] Heavens, O. S. 1960. Optical properties of thin films, *Rep. Prog. Phys.*, 23:1–65. DOI: 10.1088/0034-4885/23/1/301. 2

[14] Faryad, M. and Lakhtakia, A. 2018. *Infinite-Space Dyadic Green Functions in Electromagnetism* (San Rafael, CA, Morgan & Claypool), IOP Concise Physics. DOI: 10.1088/978-1-6817-4557-2. 2

[15] Glytsis, E. N. and Gaylord, T. K. 1987. Rigorous three-dimensional coupled-wave diffraction analysis of single and cascaded anisotropic gratings, *J. Opt. Soc. Am. A*, 4:2061–2080. DOI: 10.1364/josaa.4.002061. 3, 4

[16] Onishi, M., Crabtree, K., and Chipman, R. C. 2011. Formulation of rigorous coupled-wave theory for gratings in bianisotropic media, *J. Opt. Soc. Am. A*, 28:1747–1758. DOI: 10.1364/josaa.28.001747. 3, 4

[17] Weinstein, W. 1947. The reflectivity and transmissivity of multiple thin coatings, *J. Opt. Soc. Am.*, 37:576–581. DOI: 10.1364/josa.37.000576. 3

[18] Herpin, A. 1947. Calcul du pouvoir réflecteur d'un système stratifié quelconque, *C. R. Hebdo. Séances l'Acad. Sci.*, 225:182–183, Paris. 3

[19] Muchmore, R. B. 1948. Optimum band width for two layer anti-reflection films, *J. Opt. Soc. Am.*, 38:20–26. DOI: 10.1364/josa.38.000020. 3

[20] Abelès, F. 1950. Recherches sur la propagation des ondes électromagnétiques sinusoïdales dans les milieux stratifiés. Application aux couches minces (1re partie), *Ann. Phys.*, 5:596–640, Paris. DOI: 10.1051/anphys/195012050706. 3, 4

[21] Abelès, F. 1957. Optical properties of thin absorbing films, *J. Opt. Soc. Am.*, 47:473–482. DOI: 10.1364/josa.47.000473. 3

[22] Marcuvitz, N. and Schwinger, J. S. 1951. On the representation of the electric and magnetic fields produced by currents and discontinuities in wave guides, I, *J. Appl. Phys.*, 22:806–819. DOI: 10.1063/1.1700052. 3

[23] Weiglhofer, W. 1987. Scalarization of Maxwell's equations in general inhomogeneous bianisotropic media, *IEE Proc. H*, 134:357–360. DOI: 10.1049/ip-h-2.1987.0070. 3

[24] Billard, J. 1966. *Contribution a l'etude de la propagation des ondes electromagnetiques planes dans certains milieux materiels (2ème these)*, Ph.D. Dissertation (Université de Paris 6, France), pages 175–178. 4

[25] Keller, H. B. and Keller, J. B. 1962. Exponential-like solutions of systems of linear ordinary differential equations, *J. Soc. Indust. Appl. Math.*, 10(2):246–259. DOI: 10.1137/0110019. 4

[26] Teitler, S. and Henvis, B. W. 1970. Refraction in stratified, anisotropic media, *J. Opt. Soc. Am.*, 60:830–834. DOI: 10.1364/josa.60.000830. 4

[27] Berreman, D. W. and Scheffer, T. J. 1970. Bragg reflection of light from single-domain cholesteric liquid-crystal films, *Phys. Rev. Lett.*, 25:577–581. DOI: 10.1103/physrevlett.25.902.4. 4

[28] Berreman, D. W. 1972. Optics in stratified and anisotropic media: 4×4-matrix formulation, *J. Opt. Soc. Am.*, 62:502–510. DOI: 10.1364/josa.62.000502. 4

[29] Lakhtakia, A. 2003. Comment on 'Analytical solution of non-homogeneous anisotropic wave equations based on differential transfer matrices,' *J. Opt. A: Pure Appl. Opt.*, 5:432–433. DOI: 10.1088/1464-4258/5/4/401. 4

[30] Abdulhalim, I., Benguigui, L., and Weil, R. 1985. Selective reflection by helicoidal liquid crystals. Results of an exact calculation using the 4×4 characteristic matrix method, *J. Phys.*, 46:815–825, Paris. DOI: 10.1051/jphys:01985004605081500. 4

[31] Venugopal, V. C. and Lakhtakia, A. 1998. Dielectric sculptured nematic thin films for rugate-like filters, *Opt. Commun.*, 149:217–222. DOI: 10.1016/s0030-4018(98)00029-7. 4

[32] Venugopal, V. C. and Lakhtakia, A. 2000. Electromagnetic plane-wave response characteristics of non-axially excited slabs of dielectric thin-film helicoidal bianisotropic mediums, *Proc. R. Soc. Lond. A*, 456:125–161. DOI: 10.1098/rspa.2000.0511. 4

[33] Polo, J. A., Jr., and Lakhtakia, A. 2002. Numerical implementation of exact analytical solution for oblique propagation in a cholesteric liquid crystal, *Microw. Opt. Technol. Lett.*, 35:397–400. DOI: 10.1002/mop.10618. 4

[34] Ward, L. 2000. *The Optical Constants of Bulk Materials and Films*, 2nd ed. (Bristol, UK, Institute of Physics). 4

[35] Hodgkinson, I. J. and Wu, Q. h. 1997. *Birefringent Thin Films and Polarizing Elements* (Singapore, World Scientific). DOI: 10.1142/3324. 4

[36] MacLeod, H. A. 2001. *Thin-Film Optical Filters*, 3rd ed. (Boca Raton, FL, CRC Press). DOI: 10.1201/9781420033236. 4

[37] Baumeister, P. W. 2004. *Optical Coating Technology* (Bellingham, WA, SPIE Press). DOI: 10.1117/3.548071. 4

[38] Boardman, A. D., Ed., 1982. *Electromagnetic Surface Modes* (Chicester, UK, Wiley). 4

[39] Marchevskiĭ, F. N., Strizhevskiĭ, V. L., and Strizhevskiĭ, S. V. 1984. Singular electromagnetic waves in bounded anisotropic media, *Sov. Phys. Solid State*, 26:911–912. 4

[40] D'yakonov, M. I. 1988. New type of electromagnetic wave propagating at an interface, *Sov. Phys. JETP*, 67:714–716. 4

[41] Takayama, O., Crasovan, L., Artigas, D., and Torner, L. 2009. Observation of Dyakonov surface waves, *Phys. Rev. Lett.*, 102:043903. DOI: 10.1103/physrevlett.102.043903. 4

[42] Homola, J., Ed., 2006. *Surface Plasmon Resonance Based Sensors* (Heidelberg, Germany, Springer). DOI: 10.1007/b100321. 4, 5

[43] Pitarke, J. M., Silkin, V. M., Chulkov, E. V., and Echenique, P. M. 2007. Theory of surface plasmons and surface-plasmon polaritons, *Rep. Prog. Phys.*, 70:1–87. DOI: 10.1088/0034-4885/70/1/r01. 4

[44] Yeh, P., Yariv, A., and Hong, C.-S. 1977. Electromagnetic propagation in periodic stratified media. I. General theory, *J. Opt. Soc. Am.*, 67:423–438. DOI: 10.1364/josa.67.000423. 4

[45] Martorell, J., Sprung, D. W. L., and Morozov, G. V. 2006. Surface TE waves on 1D photonic crystals, *J. Opt. A: Pure Appl. Opt.*, 8:630–638. DOI: 10.1088/1464-4258/8/8/003. 4

[46] Lakhtakia, A. and Polo, J. A., Jr. 2007. Dyakonov–Tamm wave at the planar interface of a chiral sculptured thin film and an isotropic dielectric material, *J. Eur. Opt. Soc.—Rapid Pub.*, 2:07021. DOI: 10.2971/jeos.2007.07021. 4

[47] Pulsifer, D. P., Faryad, M., and Lakhtakia, A. 2013. Observation of the Dyakonov–Tamm wave, *Phys. Rev. Lett.*, 111:243902. DOI: 10.1103/physrevlett.111.243902. 4

[48] Chiadini, F., Fiumara, V., Scaglione, A., and Lakhtakia, A. 2016. Compound guided waves that mix characteristics of surface-plasmon-polariton, Tamm, Dyakonov–Tamm, and Uller–Zenneck waves, *J. Opt. Soc. Am. B*, 33:1197–1206. DOI: 10.1364/josab.33.001197. 4

[49] Turbadar, T. 1959. Complete absorption of light by thin metal films, *Proc. Phys. Soc.*, 73:40–44. DOI: 10.1088/0370-1328/73/1/307. 4

[50] Turbadar, T. 1964. Complete absorption of plane polarized light by thin metal films, *Opt. Acta*, 11:207–210. DOI: 10.1080/713817875. 4

[51] Kretschmann, E. and Raether, H. 1968. Radiative decay of nonradiative surface plasmons excited by light, *Z. Naturforsch. A*, 23:2135–2136. DOI: 10.1515/zna-1968-1247. 4

[52] Otto, A. 1968. Excitation of nonradiative surface plasma waves in silver by the method of frustrated total reflection, *Z. Phys.*, 216:398–410. DOI: 10.1007/bf01391532. 4

[53] Pulsifer, D. P., Faryad, M., and Lakhtakia, A. 2012. Grating-coupled excitation of Tamm waves, *J. Opt. Soc. Am. B*, 29:2260–2269. DOI: 10.1364/josab.29.002260. 5

[54] Faryad, M. and Lakhtakia, A. 2011. Multiple trains of same-color surface plasmon-polaritons guided by the planar interface of a metal and a sculptured nematic thin film. Part V: Grating-coupled excitation, *J. Nanophoton.*, 5:053527. DOI: 10.1117/1.3663210. 5

[55] Hasan, M. Z. and Kane, C. L. 2010. Topological insulators, *Rev. Mod. Phys.*, 82:3045–3067. DOI: 10.1103/RevModPhys.82.3045. 5

[56] Lakhtakia, A. and Mackay, T. G. 2016. Classical electromagnetic model of surface states in topological insulators, *J. Nanophoton.*, 10:033004. DOI: 10.1117/1.jnp.10.033004. 5

[57] Diovisalvi, A., Lakhtakia, A., Fiumara, V., and Chiadini, F. 2017. Bilaterally asymmetric reflection and transmission of light by a grating structure containing a topological insulator, *Opt. Commun.*, 398:67–76. DOI: 10.1016/j.optcom.2017.04.017. 5

[58] Depine, R. A. 2016. *Graphene Optics: Electromagnetic Solution of Canonical Problems* (San Rafael, CA, Morgan & Claypool), IOP Concise Physics. DOI: 10.1088/978-1-6817-4309-7. 5

[59] Chiadini, F., Scaglione, A., Fiumara, V., Shuba, M. V., and Lakhtakia, A. 2019. Effect of chemical potential on Dyakonov–Tamm waves guided by a graphene-coated structurally chiral medium, *J. Opt.*, 21:055002, UK. DOI: 10.1088/2040-8986/ab137f.
Chiadini, F., Scaglione, A., Fiumara, V., Shuba, M. V., and Lakhtakia, A. 2019. Effect of chemical potential on Dyakonov–Tamm waves guided by a graphene-coated structurally chiral medium, *J. Opt.*, 21:079501, UK. (erratum) DOI: 10.1088/2040-8986/ab2a57. 5

[60] Chen, H. C. 1983. *Theory of Electromagnetic Waves* (New York, McGraw-Hill). 5

CHAPTER 2

Electromagnetic Preliminaries

As a precursor to the presentation of the TMM for electromagnetic reflection–transmission boundary-value problems, the essential background electromagnetic theory is presented in this chapter. After the introduction of the Maxwell postulates, the constitutive relations are described for the most general linear materials and specializations thereof. The matter of planewave propagation in such materials is then considered, leading to the formulation of a 4×4 matrix ordinary differential equation which is the bedrock of the TMM.

2.1 MAXWELL POSTULATES

2.1.1 MICROSCOPIC PERSPECTIVE

Every material is spatially nonhomogeneous and temporally varying from the *microscopic* electromagnetic perspective, since it is a collection of point charges. Given that the approach adopted in this book is a classical one, uncertainties in the positions or velocities of these point charges are irrelevant. An ensemble of point charges q_ℓ, $\ell \in \{1, 2, 3, \ldots\}$, positioned at $\underline{r}_\ell(t)$ and moving with velocity $\underline{v}_\ell(t)$ at time t, gives rise to the microscopic charge density

$$\tilde{c}(\underline{r}, t) = \sum_\ell q_\ell \, \delta \left[\underline{r} - \underline{r}_\ell(t) \right] \tag{2.1}$$

and the microscopic current density

$$\underline{\tilde{j}}(\underline{r}, t) = \sum_\ell q_\ell \, \underline{v}_\ell \, \delta \left[\underline{r} - \underline{r}_\ell(t) \right], \tag{2.2}$$

wherein the Dirac delta satisfies the constraint

$$\int_{-\infty}^{\infty} \delta(s) \, ds = 1. \tag{2.3}$$

Both of the densities are sources of two microscopic electromagnetic fields, namely the electric field $\underline{\tilde{e}}(\underline{r}, t)$ and the magnetic field $\underline{\tilde{b}}(\underline{r}, t)$.

The relationships between the microscopic source densities, $\tilde{c}(\underline{r},t)$ and $\tilde{\underline{j}}(\underline{r},t)$, and the fields, $\tilde{\underline{e}}(\underline{r},t)$ and $\tilde{\underline{b}}(\underline{r},t)$, are encapsulated by the microscopic Maxwell postulates [1]

$$\left.\begin{aligned}
&\nabla\times\tilde{\underline{e}}(\underline{r},t)+\frac{\partial}{\partial t}\tilde{\underline{b}}(\underline{r},t)=\underline{0}\\
&\nabla\times\tilde{\underline{b}}(\underline{r},t)-\varepsilon_0\mu_0\frac{\partial}{\partial t}\tilde{\underline{e}}(\underline{r},t)=\mu_0\tilde{\underline{j}}(\underline{r},t)\\
&\underline{\nabla}\bullet\tilde{\underline{e}}(\underline{r},t)=\frac{1}{\varepsilon_0}\tilde{c}(\underline{r},t)\\
&\underline{\nabla}\bullet\tilde{\underline{b}}(\underline{r},t)=0
\end{aligned}\right\}. \tag{2.4}$$

The permittivity and permeability of matter-free space are denoted by $\varepsilon_0 = 8.854\times10^{-12}\ \mathrm{F\,m^{-1}}$ and $\mu_0 = 4\pi\times10^{-7}\ \mathrm{H\,m^{-1}}$, respectively. The microscopic fields $\tilde{\underline{e}}(\underline{r},t)$ and $\tilde{\underline{b}}(\underline{r},t)$ possess spatial variations over distances $\lesssim 10^{-10}$ m and temporal variations over durations ranging from $\lesssim 10^{-13}$ s for nuclear vibrations to $\lesssim 10^{-17}$ s for electronic orbital motion [1].

2.1.2 MACROSCOPIC PERSPECTIVE

The summation index ℓ in (2.1) and (2.2) ranges from 1 to an impractically large number in any volume occupied by a material that may be characterized from a macroscopic perspective. Consequently, it is desirable to consider the spatiotemporal averages of the microscopic quantities in (2.4), from a *macroscopic* perspective [2]. In fact, spatial averaging alone suffices since it implicitly involves temporal averaging, due to the universal maximum speed $c_0 = (\varepsilon_0\mu_0)^{-1/2}$ being finite [1]. The spatial average should be taken over volumes which are sufficiently large as to contain many point charges but the linear extent of the averaging volume should be much smaller than the smallest electromagnetic wavelength in consideration. Thus, the macroscopic perspective is appropriate for solids and liquids in the extreme-ultraviolet regime and in longer-wavelength regimes. The appropriate wavelength range for the macroscopic perspective may have a much larger lower bound in rarefied gases.

Adoption of the macroscopic perspective leads to the replacement of (2.4) by

$$\left.\begin{aligned}
&\nabla\times\tilde{\underline{E}}(\underline{r},t)+\frac{\partial}{\partial t}\tilde{\underline{B}}(\underline{r},t)=\underline{0}\\
&\nabla\times\tilde{\underline{B}}(\underline{r},t)-\varepsilon_0\mu_0\frac{\partial}{\partial t}\tilde{\underline{E}}(\underline{r},t)=\mu_0\tilde{\underline{J}}(\underline{r},t)\\
&\underline{\nabla}\bullet\tilde{\underline{E}}(\underline{r},t)=\frac{1}{\varepsilon_0}\tilde{\rho}(\underline{r},t)\\
&\underline{\nabla}\bullet\tilde{\underline{B}}(\underline{r},t)=0
\end{aligned}\right\}. \tag{2.5}$$

The macroscopic fields $\underline{\tilde{E}}(\underline{r},t)$ and $\underline{\tilde{B}}(\underline{r},t)$ represent the spatial averages of $\underline{\tilde{e}}(\underline{r},t)$ and $\underline{\tilde{b}}(\underline{r},t)$, respectively; and the macroscopic charge and current densities $\tilde{\rho}(\underline{r},t)$ and $\underline{\tilde{J}}(\underline{r},t)$ are likewise related to $\tilde{c}(\underline{r},t)$ and $\underline{\tilde{j}}(\underline{r},t)$.

The macroscopic source densities in a material may be regarded as either externally impressed or arising from internal mechanisms. Thus, these source densities can be partitioned as

$$\left.\begin{aligned}\tilde{\rho}(\underline{r},t) &= \tilde{\rho}_{\text{ext}}(\underline{r},t) + \tilde{\rho}_{\text{int}}(\underline{r},t)\\ \underline{\tilde{J}}(\underline{r},t) &= \underline{\tilde{J}}_{\text{ext}}(\underline{r},t) + \underline{\tilde{J}}_{\text{int}}(\underline{r},t)\end{aligned}\right\}, \tag{2.6}$$

wherein the subscripts "ext" and "int" identify the externally impressed and internally arising source densities, respectively. The internally arising source densities are characterized via the macroscopic polarization $\underline{\tilde{P}}(\underline{r},t)$ and magnetization $\underline{\tilde{M}}(\underline{r},t)$ as follows:

$$\left.\begin{aligned}\tilde{\rho}_{\text{int}}(\underline{r},t) &= -\underline{\nabla}\bullet\underline{\tilde{P}}(\underline{r},t)\\ \underline{\tilde{J}}_{\text{int}}(\underline{r},t) &= \frac{\partial}{\partial t}\underline{\tilde{P}}(\underline{r},t) + \frac{1}{\mu_0}\underline{\nabla}\times\underline{\tilde{M}}(\underline{r},t)\end{aligned}\right\}. \tag{2.7}$$

However, if $\underline{\tilde{P}}(\underline{r},t)$ were replaced by $\underline{\tilde{P}}(\underline{r},t) - \underline{\nabla}\times\underline{\tilde{A}}(\underline{r},t)$ and $\underline{\tilde{M}}(\underline{r},t)$ by $\underline{\tilde{M}}(\underline{r},t) + \mu_0\,(\partial/\partial t)\,\underline{\tilde{A}}(\underline{r},t)$, where $\underline{\tilde{A}}(\underline{r},t)$ is some differentiable vector function, then $\tilde{\rho}_{\text{int}}(\underline{r},t)$ and $\underline{\tilde{J}}_{\text{int}}(\underline{r},t)$ given by (2.7) would remain unchanged. Hence, a degree of ambiguity is associated with the internally arising source densities represented by (2.7).

The polarization and magnetization are subsumed into the following definitions of two macroscopic electromagnetic fields:[1]

$$\left.\begin{aligned}\underline{\tilde{D}}(\underline{r},t) &= \varepsilon_0\,\underline{\tilde{E}}(\underline{r},t) + \underline{\tilde{P}}(\underline{r},t)\\ \underline{\tilde{H}}(\underline{r},t) &= \frac{1}{\mu_0}\underline{\tilde{B}}(\underline{r},t) - \frac{1}{\mu_0}\underline{\tilde{M}}(\underline{r},t)\end{aligned}\right\}. \tag{2.8}$$

The fields $\underline{\tilde{D}}(\underline{r},t)$ and $\underline{\tilde{H}}(\underline{r},t)$ develop in a material in response to the fields $\underline{\tilde{E}}(\underline{r},t)$ and $\underline{\tilde{B}}(\underline{r},t)$. Consequently, $\underline{\tilde{D}}(\underline{r},t)$ and $\underline{\tilde{H}}(\underline{r},t)$ are regarded as *induction* fields, while $\underline{\tilde{E}}(\underline{r},t)$ and $\underline{\tilde{B}}(\underline{r},t)$ are regarded as *primitive* fields. Unlike the induction fields, the primitive fields may be measured directly via the Lorentz force [1]

$$\underline{\tilde{F}}_{\text{Lor}}(\underline{r},t) = q(\underline{r},t)\left[\underline{\tilde{E}}(\underline{r},t) + \underline{v}(\underline{r},t)\times\underline{\tilde{B}}(\underline{r},t)\right] \tag{2.9}$$

acting on a point charge $q(\underline{r},t)$ traveling at velocity $\underline{v}(\underline{r},t)$.

By substituting (2.6)–(2.8) into (2.5), the four macroscopic electromagnetic fields $\underline{\tilde{E}}(\underline{r},t)$, $\underline{\tilde{D}}(\underline{r},t)$, $\underline{\tilde{B}}(\underline{r},t)$, and $\underline{\tilde{H}}(\underline{r},t)$ are brought together in the macroscopic Maxwell postulates written

[1] An alternative convention is in common use concerning the definitions of the vectors $\underline{\tilde{J}}_{\text{int}}(\underline{r},t)$, $\underline{\tilde{M}}(\underline{r},t)$, and $\underline{\tilde{H}}(\underline{r},t)$. This convention involves $(2.7)_2$ being replaced by $\underline{\tilde{J}}_{\text{int}}(\underline{r},t) = (\partial/\partial t)\,\underline{\tilde{P}}(\underline{r},t) + \underline{\nabla}\times\underline{\tilde{M}}(\underline{r},t)$ and $(2.8)_2$ being replaced by $\underline{\tilde{H}}(\underline{r},t) = \mu_0^{-1}\underline{\tilde{B}}(\underline{r},t) - \underline{\tilde{M}}(\underline{r},t)$. The alternative convention is not used in this book.

in standard form as follows:

$$\left.\begin{aligned} \nabla \times \underline{\tilde{H}}(\underline{r},t) - \frac{\partial}{\partial t}\,\underline{\tilde{D}}(\underline{r},t) &= \underline{\tilde{J}}_{\text{ext}}(\underline{r},t) \\ \nabla \times \underline{\tilde{E}}(\underline{r},t) + \frac{\partial}{\partial t}\,\underline{\tilde{B}}(\underline{r},t) &= \underline{0} \\ \underline{\nabla} \bullet \underline{\tilde{D}}(\underline{r},t) &= \tilde{\rho}_{\text{ext}}(\underline{r},t) \\ \underline{\nabla} \bullet \underline{\tilde{B}}(\underline{r},t) &= 0 \end{aligned}\right\}. \tag{2.10}$$

These postulates comprise four linear differential equations: (i) the two homogeneous differential equations $(2.10)_2$ and $(2.10)_4$ involving the primitive fields and (ii) the two inhomogeneous differential equations $(2.10)_1$ and $(2.10)_3$ involving the induction fields.

The divergence postulate $(2.10)_4$ is completely consistent with the curl postulate $(2.10)_2$, as can be seen by taking the divergence of the left and right sides of the latter postulate. The consistency of the divergence postulate $(2.10)_3$ and the curl postulate $(2.10)_1$ mandates the reasonable constraint

$$\underline{\nabla} \bullet \underline{\tilde{J}}_{\text{ext}}(\underline{r},t) + \frac{\partial}{\partial t}\,\tilde{\rho}_{\text{ext}}(\underline{r},t) = 0. \tag{2.11}$$

The two Maxwell curl postulates suffice for our purposes in the remainder of this book, the macroscopic continuity equation (2.11) being presumed to hold in practical situations.

2.2 CONSTITUTIVE RELATIONS

Although the Maxwell postulates (2.10) govern all electromagnetic phenomenons in materials, they cannot be solved (for the primitive or the induction fields) without further information being supplied. This further information is provided by constitutive relations, which relate the primitive fields to the induction fields in the material under consideration. Formally, these may be expressed in the general form

$$\left.\begin{aligned} \underline{\tilde{D}}(\underline{r},t) &= \mathcal{F}\left\{\underline{\tilde{E}}(\underline{r},t), \underline{\tilde{B}}(\underline{r},t)\right\} \\ \underline{\tilde{H}}(\underline{r},t) &= \mathcal{G}\left\{\underline{\tilde{E}}(\underline{r},t), \underline{\tilde{B}}(\underline{r},t)\right\} \end{aligned}\right\}, \tag{2.12}$$

with $\mathcal{F}$ and $\mathcal{G}$ being linear functions of $\underline{\tilde{E}}(\underline{r},t)$ and $\underline{\tilde{B}}(\underline{r},t)$ for linear materials, and nonlinear functions of $\underline{\tilde{E}}(\underline{r},t)$ and $\underline{\tilde{B}}(\underline{r},t)$ for nonlinear materials. This book is devoted to the TMM for linear materials.

In general, a material's electromagnetic response is spatiotemporally nonlocal. Consequently, in full generality, the constitutive relations of a linear material are expressed as [3]

$$\left.\begin{aligned}\underline{\tilde{D}}(\underline{r},t) &= \int_{t'}\int_{\underline{r}'}\Big[\underline{\underline{\tilde{\varepsilon}}}_{\rm EB}(\underline{r}',t')\cdot\underline{\tilde{E}}(\underline{r}-\underline{r}',t-t') \\ &\qquad +\underline{\underline{\tilde{\xi}}}_{\rm EB}(\underline{r}',t')\cdot\underline{\tilde{B}}(\underline{r}-\underline{r}',t-t')\Big]\,d^3\underline{r}'\,dt' \\ \underline{\tilde{H}}(\underline{r},t) &= \int_{t'}\int_{\underline{r}'}\Big[\underline{\underline{\tilde{\zeta}}}_{\rm EB}(\underline{r}',t')\cdot\underline{\tilde{E}}(\underline{r}-\underline{r}',t-t') \\ &\qquad +\underline{\underline{\tilde{\nu}}}_{\rm EB}(\underline{r}',t')\cdot\underline{\tilde{B}}(\underline{r}-\underline{r}',t-t')\Big]\,d^3\underline{r}'\,dt'\end{aligned}\right\}, \tag{2.13}$$

in terms of the four 3×3 constitutive dyadics $\underline{\underline{\tilde{\varepsilon}}}_{\rm EB}(\underline{r},t)$, $\underline{\underline{\tilde{\xi}}}_{\rm EB}(\underline{r},t)$, $\underline{\underline{\tilde{\zeta}}}_{\rm EB}(\underline{r},t)$, and $\underline{\underline{\tilde{\nu}}}_{\rm EB}(\underline{r},t)$. A guide to 3×3 dyadics is provided in Appendix A.

The manifestation of nonlocality can vary greatly from one material to another. If a characteristic length scale in a material is similar to the electromagnetic wavelength, then spatial nonlocality may be significant [4]. However, the effects of spatial nonlocality are negligible in the vast majority of situations currently considered as practical. On the other hand, since electromagnetic signals travel rapidly, the effects of temporal nonlocality must not be ignored. Spatially local but temporally nonlocal linear materials are characterized by the following constitutive relations:

$$\left.\begin{aligned}\underline{\tilde{D}}(\underline{r},t) &= \int_{t'}\Big[\underline{\underline{\tilde{\varepsilon}}}_{\rm EB}(\underline{r},t')\cdot\underline{\tilde{E}}(\underline{r},t-t')+\underline{\underline{\tilde{\xi}}}_{\rm EB}(\underline{r},t')\cdot\underline{\tilde{B}}(\underline{r},t-t')\Big]\,dt' \\ \underline{\tilde{H}}(\underline{r},t) &= \int_{t'}\Big[\underline{\underline{\tilde{\zeta}}}_{\rm EB}(\underline{r},t')\cdot\underline{\tilde{E}}(\underline{r},t-t')+\underline{\underline{\tilde{\nu}}}_{\rm EB}(\underline{r},t')\cdot\underline{\tilde{B}}(\underline{r},t-t')\Big]\,dt'\end{aligned}\right\}. \tag{2.14}$$

2.3 FREQUENCY DOMAIN

The time-domain constitutive relations (2.14) are often inconvenient as the convolution integrals therein usually lead to mathematical complications that are analytically intractable and computationally challenging. These complications are bypassed by switching to the frequency domain by taking the temporal Fourier transforms of all fields and sources appearing in (2.10) and (2.14) as follows:

$$\mathcal{Z}(\underline{r},\omega)=\int_{-\infty}^{\infty}\tilde{\mathcal{Z}}(\underline{r},t)\,\exp(i\omega t)\,dt\,,\quad \mathcal{Z}\in\left\{\underline{\underline{\varepsilon}}_{\rm EB},\underline{\underline{\xi}}_{\rm EB},\underline{\underline{\zeta}}_{\rm EB},\underline{\underline{\nu}}_{\rm EB},\underline{E},\underline{D},\underline{B},\underline{H},\underline{J}_{\rm ext},\rho_{\rm ext}\right\}. \tag{2.15}$$

Here, ω is the angular frequency and $i=\sqrt{-1}$. When $\tilde{\mathcal{Z}}(\underline{r},t)$ is either a source or a field, its counterpart $\mathcal{Z}(\underline{r},\omega)$ is referred to as a *phasor*.

Accordingly, the Maxwell postulates (2.10) transform in the frequency domain to

$$\left.\begin{aligned} &\nabla \times \underline{H}(\underline{r},\omega) + i\omega \underline{D}(\underline{r},\omega) = \underline{J}_{\text{ext}}(\underline{r},\omega) \\ &\nabla \times \underline{E}(\underline{r},\omega) - i\omega \underline{B}(\underline{r},\omega) = \underline{0} \\ &\nabla \cdot \underline{D}(\underline{r},\omega) = \rho_{\text{ext}}(\underline{r},\omega) \\ &\nabla \cdot \underline{B}(\underline{r},\omega) = 0 \end{aligned}\right\} ; \tag{2.16}$$

furthermore, application of the convolution theorem [5] to (2.14) delivers the frequency-domain constitutive relations

$$\left.\begin{aligned} \underline{D}(\underline{r},\omega) &= \underline{\underline{\varepsilon}}_{\text{EB}}(\underline{r},\omega) \cdot \underline{E}(\underline{r},\omega) + \underline{\underline{\xi}}_{\text{EB}}(\underline{r},\omega) \cdot \underline{B}(\underline{r},\omega) \\ \underline{H}(\underline{r},\omega) &= \underline{\underline{\zeta}}_{\text{EB}}(\underline{r},\omega) \cdot \underline{E}(\underline{r},\omega) + \underline{\underline{\nu}}_{\text{EB}}(\underline{r},\omega) \cdot \underline{B}(\underline{r},\omega) \end{aligned}\right\} . \tag{2.17}$$

A price has to be paid for the relative simplicity of the frequency-domain constitutive relations (2.17) as compared with the time-domain constitutive relations (2.14): The electromagnetic fields and constitutive dyadics in the time-domain description (2.14) are all real-valued quantities whereas their counterparts in the frequency-domain description (2.17) are all complex valued. Thus, inverse temporal Fourier transforms must be taken to convert the frequency-domain quantities into real-valued physical quantities.

The principle of causality leads to constraints on the real and imaginary parts of the frequency-domain constitutive parameters. Since a passive material cannot respond to a stimulus until *after* the stimulus has been received, we have

$$\left.\begin{aligned} &\tilde{\underline{\underline{\varepsilon}}}_{\text{EB}}(\underline{r},t) - \varepsilon_0 \delta(t) \underline{\underline{I}} \equiv \underline{\underline{0}} \\ &\tilde{\underline{\underline{\xi}}}_{\text{EB}}(\underline{r},t) \equiv \underline{\underline{0}} \\ &\tilde{\underline{\underline{\zeta}}}_{\text{EB}}(\underline{r},t) \equiv \underline{\underline{0}} \\ &\mu_0^{-1} \delta(t) \underline{\underline{I}} - \tilde{\underline{\underline{\nu}}}_{\text{EB}}(\underline{r},t) \equiv \underline{\underline{0}} \end{aligned}\right\} \quad \text{for} \quad t \le 0 . \tag{2.18}$$

Now let the scalar function $\tilde{\mathcal{Z}}(\underline{r},t)$ represent an arbitrary component of any one of the dyadics $\tilde{\underline{\underline{\varepsilon}}}_{\text{EB}}(\underline{r},t) - \varepsilon_0 \delta(t) \underline{\underline{I}}$, $\tilde{\underline{\underline{\xi}}}_{\text{EB}}(\underline{r},t)$, $\tilde{\underline{\underline{\zeta}}}_{\text{EB}}(\underline{r},t)$, and $\mu_0^{-1}\delta(t)\underline{\underline{I}} - \tilde{\underline{\underline{\nu}}}_{\text{EB}}(\underline{r},t)$. The analytic continuation of $\mathcal{Z}(\underline{r},\omega)$ in the upper half of the complex-ω plane then yields the Hilbert transforms

$$\left.\begin{aligned} \text{Re}\,\{\mathcal{Z}(\underline{r},\omega)\} &= \frac{1}{\pi} \text{P} \int_{-\infty}^{\infty} \frac{\text{Im}\,\{\mathcal{Z}(\underline{r},s)\}}{s-\omega}\, ds \\ \text{Im}\,\{\mathcal{Z}(\underline{r},\omega)\} &= -\frac{1}{\pi} \text{P} \int_{-\infty}^{\infty} \frac{\text{Re}\,\{\mathcal{Z}(\underline{r},s)\}}{s-\omega}\, ds \end{aligned}\right\} , \tag{2.19}$$

where P signifies the Cauchy principal value. As $\tilde{\mathcal{Z}}(\underline{r},t)$ is real valued, $\mathcal{Z}(\underline{r},\omega)$ is related to its complex conjugate $\mathcal{Z}^*(\underline{r},\omega)$ by

$$\mathcal{Z}(\underline{r},-\omega) = \mathcal{Z}^*(\underline{r},\omega). \tag{2.20}$$

By exploiting the symmetry condition (2.20), the Hilbert transforms (2.19) give rise to the Kramers–Kronig relations [6]

$$\left.\begin{aligned} \text{Re}\,\{\mathcal{Z}(\underline{r},\omega)\} &= \frac{2}{\pi}\text{P}\int_0^\infty \frac{s\,\text{Im}\,\{\mathcal{Z}(\underline{r},s)\}}{s^2-\omega^2}\,ds \\ \text{Im}\,\{\mathcal{Z}(\underline{r},\omega)\} &= -\frac{2}{\pi}\text{P}\int_0^\infty \frac{\omega\,\text{Re}\,\{\mathcal{Z}(\underline{r},s)\}}{s^2-\omega^2}\,ds \end{aligned}\right\}. \tag{2.21}$$

These two relations are representative of general constraints on the frequency responses of causal linear systems [7].

The partnering of the primitive field phasors $\underline{E}(\underline{r},\omega)$ and $\underline{B}(\underline{r},\omega)$ leads to the Boys–Post formulation of the constitutive relations equations (2.17). The field phasors $\underline{E}(\underline{r},\omega)$ and $\underline{B}(\underline{r},\omega)$ are paired because their inverse temporal Fourier transforms appear in the Lorentz force. Alternatively, it can be reasonable to partner $\underline{E}(\underline{r},\omega)$ with $\underline{H}(\underline{r},\omega)$, in light of the standard boundary conditions as well as the definition of the time-averaged Poynting vector [8]. That pairing leads to the Tellegen formulation of the frequency-domain constitutive relations

$$\left.\begin{aligned} \underline{D}(\underline{r},\omega) &= \underline{\underline{\varepsilon}}_{\text{EH}}(\underline{r},\omega)\cdot\underline{E}(\underline{r},\omega) + \underline{\underline{\xi}}_{\text{EH}}(\underline{r},\omega)\cdot\underline{H}(\underline{r},\omega) \\ \underline{B}(\underline{r},\omega) &= \underline{\underline{\zeta}}_{\text{EH}}(\underline{r},\omega)\cdot\underline{E}(\underline{r},\omega) + \underline{\underline{\mu}}_{\text{EH}}(\underline{r},\omega)\cdot\underline{H}(\underline{r},\omega) \end{aligned}\right\}. \tag{2.22}$$

The constitutive dyadics in the Boys–Post equations (2.17) are related to those in the Tellegen equations (2.22) as follows [3]:

$$\left.\begin{aligned} \underline{\underline{\varepsilon}}_{\text{EH}}(\underline{r},\omega) &= \underline{\underline{\varepsilon}}_{\text{EB}}(\underline{r},\omega) - \underline{\underline{\xi}}_{\text{EB}}(\underline{r},\omega)\cdot\underline{\underline{\nu}}^{-1}_{\text{EB}}(\underline{r},\omega)\cdot\underline{\underline{\zeta}}_{\text{EB}}(\underline{r},\omega) \\ \underline{\underline{\xi}}_{\text{EH}}(\underline{r},\omega) &= \underline{\underline{\xi}}_{\text{EB}}(\underline{r},\omega)\cdot\underline{\underline{\nu}}^{-1}_{\text{EB}}(\underline{r},\omega) \\ \underline{\underline{\zeta}}_{\text{EH}}(\underline{r},\omega) &= -\underline{\underline{\nu}}^{-1}_{\text{EB}}(\underline{r},\omega)\cdot\underline{\underline{\zeta}}_{\text{EB}}(\underline{r},\omega) \\ \underline{\underline{\mu}}_{\text{EH}}(\underline{r},\omega) &= \underline{\underline{\nu}}^{-1}_{\text{EB}}(\underline{r},\omega) \end{aligned}\right\}. \tag{2.23}$$

Implicitly, the constitutive dyadic $\underline{\underline{\nu}}_{\text{EB}}(\underline{r},\omega)$ is nonsingular. Caution should be exercised here, since singular constitutive dyadics are known to occur [9], albeit rarely.

The Tellegen constitutive relations (2.22) are used in the remainder of this book. For brevity, the subscript "EH" on the constitutive dyadics is omitted. For the same reason, ω is omitted from the argument list for the electromagnetic fields and sources. Thus, the Tellegen constitutive relations are written as

$$\left.\begin{aligned} \underline{D}(\underline{r}) &= \underline{\underline{\varepsilon}}(\underline{r})\cdot\underline{E}(\underline{r}) + \underline{\underline{\xi}}(\underline{r})\cdot\underline{H}(\underline{r}) \\ \underline{B}(\underline{r}) &= \underline{\underline{\zeta}}(\underline{r})\cdot\underline{E}(\underline{r}) + \underline{\underline{\mu}}(\underline{r})\cdot\underline{H}(\underline{r}) \end{aligned}\right\}. \tag{2.24}$$

If a material is spatially homogeneous, its constitutive relations are written even more simply as

$$\left.\begin{aligned} \underline{D}(\underline{r}) &= \underline{\underline{\varepsilon}} \cdot \underline{E}(\underline{r}) + \underline{\underline{\xi}} \cdot \underline{H}(\underline{r}) \\ \underline{B}(\underline{r}) &= \underline{\underline{\zeta}} \cdot \underline{E}(\underline{r}) + \underline{\underline{\mu}} \cdot \underline{H}(\underline{r}) \end{aligned}\right\} . \tag{2.25}$$

2.4 CONSTITUTIVE DYADICS

As is clear from the Tellegen constitutive relations (2.25), the most general linear homogeneous material is characterized by four 3×3 constitutive dyadics—namely, the permittivity dyadic $\underline{\underline{\varepsilon}}$, the permeability dyadic $\underline{\underline{\mu}}$, and the two magnetoelectric dyadics $\underline{\underline{\xi}}$ and $\underline{\underline{\zeta}}$. Thus, a total of 36 complex-valued constitutive parameters specify a general linear material. Spacetime symmetries greatly reduce the dimensionality of the constitutive-parameter space for many materials of interest [10], as illustrated in the following subsections.

2.4.1 ISOTROPIC AND BI-ISOTROPIC MATERIALS

In isotropic dielectric-magnetic materials, the induction fields are aligned wholly parallel to the primitive fields. Hence, their constitutive dyadics are of the form

$$\left.\begin{aligned} \underline{\underline{\varepsilon}} &= \varepsilon \underline{\underline{I}} \\ \underline{\underline{\xi}} &= \underline{\underline{0}} \\ \underline{\underline{\zeta}} &= \underline{\underline{0}} \\ \underline{\underline{\mu}} &= \mu \underline{\underline{I}} \end{aligned}\right\} , \qquad \varepsilon \in \mathbb{C}, \quad \mu \in \mathbb{C}, \tag{2.26}$$

where $\mathbb{C}$ is the set of all complex numbers. Furthermore, $\mu = \mu_0$ for isotropic dielectric materials and $\varepsilon = \varepsilon_0$ for isotropic magnetic materials.

A bi-isotropic material displays both isotropy and magnetoelectric coupling. The constitutive dyadics of bi-isotropic materials are of the form

$$\left.\begin{aligned} \underline{\underline{\varepsilon}} &= \varepsilon \underline{\underline{I}} \\ \underline{\underline{\xi}} &= \xi \underline{\underline{I}} \\ \underline{\underline{\zeta}} &= \zeta \underline{\underline{I}} \\ \underline{\underline{\mu}} &= \mu \underline{\underline{I}} \end{aligned}\right\} , \qquad \varepsilon \in \mathbb{C}, \quad \xi \in \mathbb{C}, \quad \zeta \in \mathbb{C}, \quad \mu \in \mathbb{C} . \tag{2.27}$$

An important special case occurs if $\xi = -\zeta \neq 0$; then the material is an isotropic chiral material or a reciprocal bi-isotropic material [11]. The *optical activity* of such materials can be harnessed to discriminate between left-handed and right-handed electromagnetic fields [12]. The case $\xi = \zeta \neq 0$ is also a notable one, at least from a theoretical standpoint. This is the case for topological

insulators [13], but it is physically appropriate to incorporate surface states leading to jump conditions across interfaces and setting $\xi = \zeta = 0$ [14].

Although the 3×3 constitutive dyadics of bi-isotropic materials are simply scalar multiples of $\underline{\underline{I}}$, the induction fields are generally not aligned with the primitive fields in these materials, unlike in isotropic dielectric-magnetic materials. However, key electromagnetic characteristics, such as those pertaining to planewave propagation, are independent of direction in bi-isotropic materials.

2.4.2 ANISOTROPIC AND BIANISOTROPIC MATERIALS

Many naturally occurring and engineered materials exhibit anisotropy, i.e., direction-dependent characteristics [15]. Nontrivial dyadics—as opposed to dyadics that are simply scalar multiples of $\underline{\underline{I}}$—are needed to relate the induction field phasors to the primitive field phasors for such materials.

In an anisotropic dielectric-magnetic material, the induction field $\underline{D}$ is anisotropically coupled to the primitive field $\underline{E}$ and/or the induction field $\underline{H}$ is anisotropically coupled to the primitive field $\underline{B}$. Hence, the constitutive dyadics obey the following constraints:

$$\left.\begin{array}{l} \underline{\underline{\varepsilon}} \neq \varepsilon \underline{\underline{I}} \\ \underline{\underline{\xi}} = \underline{\underline{0}} \\ \underline{\underline{\zeta}} = \underline{\underline{0}} \\ \underline{\underline{\mu}} \neq \mu \underline{\underline{I}} \end{array}\right\} . \tag{2.28}$$

Whereas $\underline{\underline{\mu}} = \mu_0 \underline{\underline{I}}$ for an anisotropic dielectric material, $\underline{\underline{\varepsilon}} = \varepsilon_0 \underline{\underline{I}}$ for an anisotropic magnetic material. For a general anisotropic dielectric-magnetic material, the non-trivial constitutive dyadics may be represented by the 3×3 Cartesian matrixes

$$\left.\begin{array}{l} \underline{\underline{\varepsilon}} = \left[\begin{array}{ccc} \varepsilon_{xx} & \varepsilon_{xy} & \varepsilon_{xz} \\ \varepsilon_{yx} & \varepsilon_{yy} & \varepsilon_{yz} \\ \varepsilon_{zx} & \varepsilon_{zy} & \varepsilon_{zz} \end{array}\right] \\ \underline{\underline{\mu}} = \left[\begin{array}{ccc} \mu_{xx} & \mu_{xy} & \mu_{xz} \\ \mu_{yx} & \mu_{yy} & \mu_{yz} \\ \mu_{zx} & \mu_{zy} & \mu_{zz} \end{array}\right] \end{array}\right\} , \tag{2.29}$$

with all matrix entries being complex valued.

The natural generalization of anisotropy is bianisotropy. In a bianisotropic material, both induction fields $\underline{D}$ and $\underline{H}$ are anisotropically coupled to both primitive fields $\underline{E}$ and $\underline{B}$. Thus,

the constitutive dyadics for a bianisotropic material satisfy

$$\left.\begin{aligned} \underline{\underline{\varepsilon}} &\neq \varepsilon \underline{\underline{I}} \\ \underline{\underline{\xi}} &\neq \xi \underline{\underline{I}} \\ \underline{\underline{\zeta}} &\neq \zeta \underline{\underline{I}} \\ \underline{\underline{\mu}} &\neq \mu \underline{\underline{I}} \end{aligned}\right\} . \tag{2.30}$$

For a general bianisotropic material, the constitutive dyadics may be represented by the 3×3 Cartesian matrixes (2.29) together with

$$\left.\begin{aligned} \underline{\underline{\xi}} &= \left[\begin{array}{ccc} \xi_{xx} & \xi_{xy} & \xi_{xz} \\ \xi_{yx} & \xi_{yy} & \xi_{yz} \\ \xi_{zx} & \xi_{zy} & \xi_{zz} \end{array}\right] \\ \underline{\underline{\zeta}} &= \left[\begin{array}{ccc} \zeta_{xx} & \zeta_{xy} & \zeta_{xz} \\ \zeta_{yx} & \zeta_{yy} & \zeta_{yz} \\ \zeta_{zx} & \zeta_{zy} & \zeta_{zz} \end{array}\right] \end{aligned}\right\} , \tag{2.31}$$

with all matrix entries being complex valued.

The structures of the constitutive dyadics in (2.28) and (2.30) reflect underlying spacetime symmetries of the materials being characterized. These symmetries are conventionally classified in terms of 122 discrete magnetic point groups and 21 continuous magnetic point groups (which encompass the symmetries of isotropic and bi-isotropic materials as degenerate cases) [10, 16–18]. The magnetic point group with the lowest symmetry, namely $\mathbf{C}_1$ in the Schoenflies notation, is especially noteworthy. For materials in this magnetic point group, the structures of the four constitutive dyadics $\underline{\underline{\varepsilon}}$, $\underline{\underline{\xi}}$, $\underline{\underline{\zeta}}$, and $\underline{\underline{\mu}}$ are completely arbitrary; i.e., a total of 36 complex-valued constitutive scalars are necessary. However, most commonly encountered anisotropic and bianisotropic materials exhibit substantial degrees of spacetime symmetry and, accordingly, far fewer constitutive scalars are needed to characterize them.

The simplest form of anisotropy is exemplified by uniaxial materials, for which the constitutive dyadics take the form

$$\underline{\underline{\sigma}} = \sigma_1 \underline{\underline{I}} + \sigma_2 \underline{u}_{\mathrm{m}}\, \underline{u}_{\mathrm{m}}, \qquad \sigma_1 \in \mathbb{C}, \quad \sigma_2 \in \mathbb{C}, \quad \sigma \in \{\varepsilon, \xi, \zeta, \mu\} \, . \tag{2.32}$$

There is just one distinguished direction, identified by the unit vector $\underline{u}_{\mathrm{m}}$. In *crystal optics*, a uniaxial dielectric material is characterized by

$$\left.\begin{aligned} \underline{\underline{\varepsilon}} &= \varepsilon_1 \underline{\underline{I}} + \varepsilon_2 \underline{u}_{\mathrm{m}}\, \underline{u}_{\mathrm{m}} \\ \underline{\underline{\xi}} &= \underline{\underline{0}} \\ \underline{\underline{\zeta}} &= \underline{\underline{0}} \\ \underline{\underline{\mu}} &= \mu_0 \underline{\underline{I}} \end{aligned}\right\} , \qquad \varepsilon_1 \in \mathbb{R}, \quad \varepsilon_2 \in \mathbb{R} \, , \tag{2.33}$$

with $\underline{u}_{\rm m}$ pointing in the direction of the *optic axis* [8] and $\mathbb{R}$ being the set of all real numbers. That is, $\pm\underline{u}_{\rm m}$ identify the special directions along which plane waves propagate with only one phase speed. Parenthetically, $\underline{u}_{\rm m}$ is also aligned with the *optic ray axis* that represents the special direction along which plane waves propagate with only one energy speed [19].

On generalizing the anisotropy represented in (2.32), constitutive dyadics of the form

$$\begin{aligned} \underline{\underline{\sigma}} &= \sigma_1 \underline{\underline{I}} + \sigma_2 \underline{u}_{\rm m}\,\underline{u}_{\rm m} + \sigma_3 \underline{u}_{\rm n}\,\underline{u}_{\rm n}, \\ &\qquad \sigma_1 \in \mathbb{C}, \quad \sigma_2 \in \mathbb{C}, \quad \sigma_3 \in \mathbb{C}, \quad \sigma \in \{\varepsilon, \xi, \zeta, \mu\}\,, \end{aligned} \tag{2.34}$$

emerge. These constitutive dyadics characterize orthorhombic biaxial materials. Herein the unit vectors $\underline{u}_{\rm m}$ and $\underline{u}_{\rm n}$ are mutually orthogonal. There are two distinguished directions here but the formulation (2.34) is not particularly insightful, as a physical interpretation of $\underline{u}_{\rm m}$ and $\underline{u}_{\rm n}$ is not readily forthcoming. The distinguished directions may be better appreciated by considering the following alternative formulation: for example, an orthorhombic dielectric material that is neither dissipative nor active may be characterized by [8, 20]

$$\left.\begin{aligned} \underline{\underline{\varepsilon}} &= \varepsilon_{\rm p} \underline{\underline{I}} + \varepsilon_{\rm q} \left(\underline{u}_{\rm p}\,\underline{u}_{\rm q} + \underline{u}_{\rm q}\,\underline{u}_{\rm p}\right) \\ \underline{\underline{\xi}} &= \underline{\underline{0}} \\ \underline{\underline{\zeta}} &= \underline{\underline{0}} \\ \underline{\underline{\mu}} &= \mu_0 \underline{\underline{I}} \end{aligned}\right\}, \qquad \varepsilon_{\rm p} \in \mathbb{R}, \quad \varepsilon_{\rm q} \in \mathbb{R}\,. \tag{2.35}$$

The unit vectors $\underline{u}_{\rm p}$ and $\underline{u}_{\rm q}$ herein are aligned with the optic ray axes [21]; that is, they are aligned with the two directions along which plane waves propagate with only one energy speed. Notice that in the case of biaxial dielectric materials the two optic ray axes do not generally coincide with the two optic axes (which represent the directions along which plane waves propagate with only one phase speed) [10, 19].

The uniaxial and biaxial constitutive dyadics present in (2.32) and (2.34) are symmetric. Antisymmetric constitutive dyadics are also commonly encountered, notably in the context of gyrotropic materials which are characterized by constitutive dyadics of the form

$$\begin{aligned} \underline{\underline{\sigma}} &= \sigma_1 \underline{\underline{I}} + \sigma_2 \underline{u}_{\rm m}\,\underline{u}_{\rm m} + \sigma_3 \underline{u}_{\rm m} \times \underline{\underline{I}}, \\ &\qquad \sigma_1 \in \mathbb{C}, \quad \sigma_2 \in \mathbb{C}, \quad \sigma_3 \in \mathbb{C}, \quad \sigma \in \{\varepsilon, \xi, \zeta, \mu\}\,. \end{aligned} \tag{2.36}$$

For example, a nondissipative magnetically biased ferrite may characterized by [22]

$$\left.\begin{aligned} \underline{\underline{\varepsilon}} &= \varepsilon_0 \underline{\underline{I}} \\ \underline{\underline{\xi}} &= \underline{\underline{0}} \\ \underline{\underline{\zeta}} &= \underline{\underline{0}} \\ \underline{\underline{\mu}} &= \mu_1 \underline{\underline{I}} + \mu_2 \underline{u}_{\rm m}\,\underline{u}_{\rm m} + i\mu_3 \underline{u}_{\rm m} \times \underline{\underline{I}} \end{aligned}\right\}, \qquad \mu_1 \in \mathbb{R}, \quad \mu_2 \in \mathbb{R}, \quad \mu_2 \in \mathbb{R}\,, \tag{2.37}$$

where the unit vector $\underline{u}_{\rm m}$ is aligned with the direction of the biasing magnetic field. An example of gyrotropy in a bianisotropic setting arises in the case of Faraday chiral materials. These are characterized by constitutive dyadics of the form [23]

$$\left.\begin{aligned} \underline{\underline{\varepsilon}} &= \varepsilon_1 \underline{\underline{I}} + \varepsilon_2 \underline{u}_{\rm m}\,\underline{u}_{\rm m} + i\varepsilon_3 \underline{u}_{\rm m} \times \underline{\underline{I}} \\ \underline{\underline{\xi}} &= i\left(\xi_1 \underline{\underline{I}} + \xi_2 \underline{u}_{\rm m}\,\underline{u}_{\rm m} + i\xi_3 \underline{u}_{\rm m} \times \underline{\underline{I}}\right) \\ \underline{\underline{\zeta}} &= -\underline{\underline{\xi}} \\ \underline{\underline{\mu}} &= \mu_1 \underline{\underline{I}} + \mu_2 \underline{u}_{\rm m}\,\underline{u}_{\rm m} + i\mu_3 \underline{u}_{\rm m} \times \underline{\underline{I}} \end{aligned}\right\}, \tag{2.38}$$

$$\sigma_1 \in \mathbb{R}, \quad \sigma_2 \in \mathbb{R}, \quad \sigma_2 \in \mathbb{R}, \quad \sigma \in \{\varepsilon, \xi, \mu\}, \tag{2.39}$$

in the absence of dissipation. For dissipative Faraday chiral materials, the constitutive parameters σ_1, σ_2, and σ_3, $\sigma \in \{\varepsilon, \xi, \mu\}$, are complex valued.

Naturally occurring materials which exhibit appreciable bianisotropic effects, under normal environmental conditions, are relatively scarce. However, artificial materials with substantial bianisotropic effects may be readily realized. Such materials can be conceptualized as homogenized composite materials, arising from constituent materials which are not themselves bianisotropic (or even anisotropic in some cases) [24].

Far from being an esoteric property, bianisotropy is actually a ubiquitous one [10]. From the perspective of special relativity, isotropy is not invariant under the Lorentz transformation. For example, a material which is an isotropic dielectric material with respect to one inertial reference frame is a bianisotropic material with respect to another inertial reference frame. Furthermore, from the perspective of general relativity, free space subjected to a gravitational field is electromagnetically equivalent to a nonhomogeneous bianisotropic material [25, 26].

2.5 WAVE PROPAGATION

Let us consider wave propagation in a homogeneous bianisotropic material described by the constitutive relations (2.25), with constitutive dyadics (2.29) and (2.30). Suppose that the spatial variation of all field phasors is of the form $\exp\left[iq(x\cos\psi + y\sin\psi)\right]$ in the xy plane, with q being a complex-valued wavenumber and the angle $\psi \in [0, 2\pi)$. In particular, the field phasors are expressed as

$$\left.\begin{aligned} \underline{E}(\underline{r}) &= \underline{e}(z)\,\exp\left[iq(x\cos\psi + y\sin\psi)\right] \\ \underline{H}(\underline{r}) &= \underline{h}(z)\,\exp\left[iq(x\cos\psi + y\sin\psi)\right] \end{aligned}\right\}, \tag{2.40}$$

with auxiliary phasors

$$\left.\begin{aligned} \underline{e}(z) &= e_x(z)\underline{u}_{\rm x} + e_y(z)\underline{u}_{\rm y} + e_z(z)\underline{u}_{\rm z} \\ \underline{h}(z) &= h_x(z)\underline{u}_{\rm x} + h_y(z)\underline{u}_{\rm y} + h_z(z)\underline{u}_{\rm z} \end{aligned}\right\}. \tag{2.41}$$

The spatial variation along the z axis will be determined in due course. In the absence of sources, propagation is dictated by the frequency-domain Maxwell curl postulates $(2.16)_{1,2}$ with $\underline{J}_{\text{ext}}(\underline{r}) \equiv \underline{0}$.

2.5.1 MATRIX ORDINARY DIFFERENTIAL EQUATION

The combination of the constitutive relations (2.25) and the source-free counterparts of the frequency-domain Maxwell curl postulates $(2.16)_{1,2}$, together with the field phasor representation (2.40), delivers the system of four coupled ordinary differential equations

$$\left.\begin{aligned}
\frac{d}{dz}e_x(z) = \;& i\omega\Big[\zeta_{yx}e_x(z) + \zeta_{yy}e_y(z) + \Big(\zeta_{yz} + \frac{q}{\omega}\cos\psi\Big)e_z(z) \\
& + \mu_{yx}h_x(z) + \mu_{yy}h_y(z) + \mu_{yz}h_z(z)\Big] \\
\frac{d}{dz}e_y(z) = \;& -i\omega\Big[\zeta_{xx}e_x(z) + \zeta_{xy}e_y(z) + \Big(\zeta_{xz} - \frac{q}{\omega}\sin\psi\Big)e_z(z) \\
& + \mu_{xx}h_x(z) + \mu_{xy}h_y(z) + \mu_{xz}h_z(z)\Big] \\
\frac{d}{dz}h_x(z) = \;& -i\omega\Big[\varepsilon_{yx}e_x(z) + \varepsilon_{yy}e_y(z) + \varepsilon_{yz}e_z(z) \\
& + \xi_{yx}h_x(z) + \xi_{yy}h_y(z) + \Big(\xi_{yz} - \frac{q}{\omega}\cos\psi\Big)h_z(z)\Big] \\
\frac{d}{dz}h_y(z) = \;& i\omega\Big[\varepsilon_{xx}e_x(z) + \varepsilon_{xy}e_y(z) + \varepsilon_{xz}e_z(z) \\
& + \xi_{xx}h_x(z) + \xi_{xy}h_y(z) + \Big(\xi_{xz} + \frac{q}{\omega}\sin\psi\Big)h_z(z)\Big]
\end{aligned}\right\}, \tag{2.42}$$

as well as the two algebraic equations

$$\left.\begin{aligned}
\varepsilon_{zz}e_z(z) + \xi_{zz}h_z(z) = \;& -\varepsilon_{zx}e_x(z) - \varepsilon_{zy}e_y(z) \\
& -\Big(\xi_{zx} - \frac{q}{\omega}\sin\psi\Big)h_x(z) - \Big(\xi_{zy} + \frac{q}{\omega}\cos\psi\Big)h_y(z) \\
\zeta_{zz}e_z(z) + \mu_{zz}h_z(z) = \;& -\Big(\zeta_{zx} + \frac{q}{\omega}\sin\psi\Big)e_x(z) - \Big(\zeta_{zy} - \frac{q}{\omega}\cos\psi\Big)e_y(z) \\
& -\mu_{zx}h_x(z) - \mu_{zy}h_y(z)
\end{aligned}\right\}. \tag{2.43}$$

Provided that the remote possibility of

$$\varepsilon_{zz}\mu_{zz} = \xi_{zz}\zeta_{zz} \tag{2.44}$$

is discounted, the two algebraic equations (2.43) may be solved to obtain the following explicit expressions for the z-directed components of the auxiliary phasors:

$$\left.\begin{aligned}
e_z(z) &= \nu_{zx}^{ee}e_x(z) + \nu_{zy}^{ee}e_y(z) + \nu_{zx}^{eh}h_x(z) + \nu_{zy}^{eh}h_y(z) \\
h_z(z) &= \nu_{zx}^{he}e_x(z) + \nu_{zy}^{he}e_y(z) + \nu_{zx}^{hh}h_x(z) + \nu_{zy}^{hh}h_y(z)
\end{aligned}\right\}. \tag{2.45}$$

Herein, the coefficients

$$\left.\begin{aligned}
\nu_{zx}^{ee} &= -\frac{\mu_{zz}\varepsilon_{zx} - \xi_{zz}\left[\zeta_{zx} + (q/\omega)\sin\psi\right]}{\varepsilon_{zz}\mu_{zz} - \xi_{zz}\zeta_{zz}} \\
\nu_{zy}^{ee} &= -\frac{\mu_{zz}\varepsilon_{zy} - \xi_{zz}\left[\zeta_{zy} - (q/\omega)\cos\psi\right]}{\varepsilon_{zz}\mu_{zz} - \xi_{zz}\zeta_{zz}} \\
\nu_{zx}^{eh} &= \frac{\xi_{zz}\mu_{zx} - \mu_{zz}\left[\xi_{zx} - (q/\omega)\sin\psi\right]}{\varepsilon_{zz}\mu_{zz} - \xi_{zz}\zeta_{zz}} \\
\nu_{zy}^{eh} &= \frac{\xi_{zz}\mu_{zy} - \mu_{zz}\left[\xi_{zy} + (q/\omega)\cos\psi\right]}{\varepsilon_{zz}\mu_{zz} - \xi_{zz}\zeta_{zz}} \\
\nu_{zx}^{he} &= \frac{\zeta_{zz}\varepsilon_{zx} - \varepsilon_{zz}\left[\zeta_{zx} + (q/\omega)\sin\psi\right]}{\varepsilon_{zz}\mu_{zz} - \xi_{zz}\zeta_{zz}} \\
\nu_{zy}^{he} &= \frac{\zeta_{zz}\varepsilon_{zy} - \varepsilon_{zz}\left[\zeta_{zy} - (q/\omega)\cos\psi\right]}{\varepsilon_{zz}\mu_{zz} - \xi_{zz}\zeta_{zz}} \\
\nu_{zx}^{hh} &= -\frac{\varepsilon_{zz}\mu_{zx} - \zeta_{zz}\left[\xi_{zx} - (q/\omega)\sin\psi\right]}{\varepsilon_{zz}\mu_{zz} - \xi_{zz}\zeta_{zz}} \\
\nu_{zy}^{hh} &= -\frac{\varepsilon_{zz}\mu_{zy} - \zeta_{zz}\left[\xi_{zy} + (q/\omega)\cos\psi\right]}{\varepsilon_{zz}\mu_{zz} - \xi_{zz}\zeta_{zz}}
\end{aligned}\right\} . \tag{2.46}$$

The explicit expressions for $e_z(z)$ and $h_z(z)$ given in (2.45) may be substituted into the system of ordinary differential equations (2.42) to obtain the 4×4 matrix ordinary differential equation

$$\frac{d}{dz}\left[\underline{f}(z)\right] = i\left[\underline{\underline{P}}\right] \cdot \left[\underline{f}(z)\right] . \tag{2.47}$$

Herein, the 4-column vector

$$\left[\underline{f}(z)\right] = \begin{bmatrix} e_x(z) \\ e_y(z) \\ h_x(z) \\ h_y(z) \end{bmatrix} , \tag{2.48}$$

while the 4×4 matrix

$$\left[\underline{\underline{P}}\right] = \omega \left(\begin{bmatrix} \zeta_{yx} & \zeta_{yy} & \mu_{yx} & \mu_{yy} \\ -\zeta_{xx} & -\zeta_{xy} & -\mu_{xx} & -\mu_{xy} \\ -\varepsilon_{yx} & -\varepsilon_{yy} & -\xi_{yx} & -\xi_{yy} \\ \varepsilon_{xx} & \varepsilon_{xy} & \xi_{xx} & \xi_{xy} \end{bmatrix} + \right.$$
$$\begin{bmatrix} \zeta_{yz} + \dfrac{q}{\omega}\cos\psi & 0 & 0 & 0 \\ 0 & -\zeta_{xz} + \dfrac{q}{\omega}\sin\psi & 0 & 0 \\ 0 & 0 & -\varepsilon_{yz} & 0 \\ 0 & 0 & 0 & \varepsilon_{xz} \end{bmatrix} \cdot \left[\underline{\underline{J}}\right] \cdot \begin{bmatrix} \nu_{zx}^{ee} & 0 & 0 & 0 \\ 0 & \nu_{zy}^{ee} & 0 & 0 \\ 0 & 0 & \nu_{zx}^{eh} & 0 \\ 0 & 0 & 0 & \nu_{zy}^{eh} \end{bmatrix} +$$
$$\left. \begin{bmatrix} \mu_{yz} & 0 & 0 & 0 \\ 0 & -\mu_{xz} & 0 & 0 \\ 0 & 0 & -\xi_{yz} + \dfrac{q}{\omega}\cos\psi & 0 \\ 0 & 0 & 0 & \xi_{xz} + \dfrac{q}{\omega}\sin\psi \end{bmatrix} \cdot \left[\underline{\underline{J}}\right] \cdot \begin{bmatrix} \nu_{zx}^{he} & 0 & 0 & 0 \\ 0 & \nu_{zy}^{he} & 0 & 0 \\ 0 & 0 & \nu_{zx}^{hh} & 0 \\ 0 & 0 & 0 & \nu_{zy}^{hh} \end{bmatrix} \right) \tag{2.49}$$

is expressed using the 4×4 matrix

$$\left[\underline{\underline{J}}\right] = \begin{bmatrix} 1 & 1 & 1 & 1 \\ 1 & 1 & 1 & 1 \\ 1 & 1 & 1 & 1 \\ 1 & 1 & 1 & 1 \end{bmatrix}. \tag{2.50}$$

2.5.2 TRANSFER MATRIX

Since the bianisotropic material under consideration is homogeneous, the matrix $\left[\underline{\underline{P}}\right]$ on the right side of (2.47) does not depend upon z (or indeed x and y). Accordingly, the solution of (2.47) is given as [27]

$$\left[\underline{f}(z)\right] = \exp\left\{i\left[\underline{\underline{P}}\right]z\right\} \cdot \left[\underline{f}(0)\right] \tag{2.51}$$

when the boundary value of $\left[\underline{f}(z)\right]$ is specified at $z = 0$. The matrizant

$$\left[\underline{\underline{M}}(z)\right] = \exp\left\{i\left[\underline{\underline{P}}\right]z\right\} \tag{2.52}$$

satisfies the matrix ordinary differential equation

$$\frac{d}{dz}\left[\underline{\underline{M}}(z)\right] = i\left[\underline{\underline{P}}\right] \cdot \left[\underline{\underline{M}}(z)\right] \tag{2.53}$$

subject to the boundary condition

$$\left[\underline{\underline{M}}(0)\right] = \left[\underline{\underline{I}}\right], \tag{2.54}$$